Probing of Coenzyme Quinone Binding Site of Mitochondrial NADH:CoQ Reductase by Fluorescence Dynamics

Ishak Ahmed and G. Krishnamoorthy*

Chemical Physics Group, Tata Institute of Fundamental Research, Homi Bhabha Road, Bombay 400 005, India

Received February 15, 1994; Revised Manuscript Received May 3, 1994®

ABSTRACT: The coenzyme quinone (CoQ) binding region of mitochondrial NADH:CoQ reductase (complex-I) was investigated by the fluorescent probes erythrosine-5′-iodoacetamide (ER) and 3,3′-diethyloxadicarbocyanine iodide (DODCI). Both steady-state and time-resolved fluorescence was used in these experiments. Both probes competed for the binding site of 2,3-dimethoxy-5-methyl-6-decyl-1,4-benzoquinone (DB), an analogue of CoQ. The fluorescence lifetimes of the complex-I bound probes were ~600 ps and ~1.7 ns in the cases of ER and DODCI, respectively. Binding of the probes was not affected by the binding of the inhibitor rotenone. However, rotenone binding caused some changes in the lifetime of the bound probes. Reduction of the enzyme caused an increase in the level of binding of ER and a decrease in the level of binding of DODCI. The level of binding of cationic DODCI increased with the increase in pH, and in the case of anionic ER the trend was reverse. Binding of Ca^{2+} to complex-I resulted in an increase in the level of binding of ER and a decrease in the level of binding of DODCI. Reaction with *N,N′*-dicyclohexylcarbodiimide (DCCD) resulted in alterations in the time-resolved fluorescence profiles of dye:complex-I system. All these results were interpreted as due to the presence of carboxyl group(s) with pK_a ~6 in the probe/CoQ binding region. The rotational correlation time (τ_r) of DODCI bound at the CoQ region was 2–3 ns. This suggested the presence of a high level of segmental mobility in the CoQ region. Reaction with DCCD increased the value of τ_r, suggesting a correlation between segmental mobility and the proton pumping activity.

NADH:CoQ reductase (EC 1.6.5.3, complex-I) is an integral multisubunit enzyme complex found in the mitochondrial inner membrane. It is also the least understood segment of the electron transport chain (for reviews see Ragan, 1987; Weiss et al., 1991; Walker, 1992; Pilkington et al., 1993). It couples the transfer of electrons from NADH to coenzyme quinone (CoQ[1]) to the transport of protons across mitochondrial inner membrane. The mammalian complex-I is composed of some 40 different subunits with a total molecular mass of approximately 700 kDa (Weiss et al., 1991; Walker et al., 1992, 1993). Seven of the subunits are encoded in the mitochondrial genome and the rest in the nuclear genome (Tuschen et al., 1990). One FMN, 4–5 Fe–S clusters, and probably one form of bound quinone (Hofhaus et al., 1991) participate in the electron-transfer pathway through the enzyme. In bovine complex-I, the Fe–S centers N-1, N-3, and N-4 form a nearly isopotential group with midpoint potential around −250 mV while the Fe–S center N-2 has a more positive potential of −30 mV (Ohnishi, 1979; Krishnamoorthy & Hinkle, 1988).

The stoichiometry of proton pumping by this enzyme has been taken as 4–5 $H^+/2e^-$ based on results from both kinetic and thermodynamic poising experiments (Lemasters et al., 1984; Wikstrom, 1984). Elucidation of the molecular mechanism of energy coupling requires information on the pathway of the electron flow and the site of proton pumping. Earlier work using inhibitors had suggested that the electron-transfer sequence through the Fe–S centers is N–1 to (N-3, N-4) to N-2, with a branching at the middle (Krishnamoorthy & Hinkle, 1988). Measurements of redox levels during steady-state electron flow and during ATP-driven reverse electron flow had indicated that the major coupling site lies between N-2 and the low potential centers N-1, N-3, and N-4 (Krishnamoorthy & Hinkle, 1988).

Two-dimensional electron microscopy and image reconstruction of the enzyme from *Neurospora crassa* have shown that the enzyme complex has an L-shaped structure with two arms at right angles to each other (Hofhaus et al., 1991). One of the arms (called the "vertical arm") protrudes into the mitochondrial matrix and houses the NADH binding site and the Fe–S centers N-1, N-3, and N-4. The other arm called the "horizontal arm" is embedded into the inner membrane and houses N-2 and the CoQ binding site. The vertical arm has been suggested to be the small form of the enzyme synthesized in chloramphenicol-inhibited cells (Hofhaus et al., 1991). The small form of the enzyme has all the redox centers except the Fe–S center N-2 and the inhibitor rotenone binding site (Wang et al., 1991). Earlier studies had shown that N-4 is accessible only from the matrix side (NADH binding side) of the inner membrane (Krishnamoorthy & Hinkle, 1988).

The rotenone binding site is quite significant in the proton pumping mechanism. This is due to the fact that only rotenone-sensitive electron-transfer reactions drive the proton pump (Ragan, 1976). Inhibition by another inhibitor capsaicin has been correlated with the presence of an energy coupling site in various organisms (Yagi, 1990). These inhibitors are generally assumed to bind to the CoQ binding site. It is quite likely that the proton pumping machinery is also close to the CoQ/inhibitor binding site which is a part of the membrane-

® Abstract published in *Advance ACS Abstracts,* July 1, 1994.

[1] Abbreviations: complex-I, NADH:CoQ reductase; CoQ, coenzyme quinone; DB, 2,3-dimethoxy-5-methyl-6-decyl-1,4-benzoquinone; DCCD, *N,N′*-dicylohexylcarbodiimide; DODCI, 3,3′-diethyloxadicarbocyanine iodide; ER, Erythrosine-5′-iodoacetamide; Fe–S, iron sulfur center; FMN, flavin mononuceotide; MES, 2-(*N*-morpholino)ethanesulfonic acid; MOPS, 3-(*N*-morpholino)propanesulfonic acid; P-DB, 2,3-dimethoxy-5-methyl-1,4-benzoquinone; SMP, submitochondrial particles; Tris, tris-(hydroxymethyl)aminoethane.

0006-2960/94/0433-9675$04.50/0 © 1994 American Chemical Society

embedded segment of the enzyme (Hofhaus et al., 1991). A recent report (Tan et al., 1993) on quinone binding in mitochondria has shown similarities in quinone binding sites in complex-I and complex-III (cytochrome bc_1 complex). Since the mechanism of proton pumping in complex-III has been accepted as the proton motive Q-cycle (Trumpower, 1990), it is tempting to look at the CoQ binding site in complex-I as a possible site of proton pumping.

We have been studying the CoQ binding site of complex-I using the fluorescent probe, erythrosine-5′-iodoacetamide (ER). This study has revealed the nonequivalent nature of sites of binding of CoQ and rotenone (Ahmed & Krishnamoorthy, 1992). In order to gain more insight into the proton pumping machinery we have probed further into this region with ER and another fluorescent probe DODCI. We have used both steady-state and time-resolved fluorescence measurements in these investigations. Our studies have revealed some intersting information on this region of the enzyme. We have also identified some probable components of the proton pumping machinery.

MATERIALS AND METHODS

Enzyme Preparations and Assay of Activity. Complex-I was prepared from beef heart mitochondria according to Hatefi & Rieske (1967). SMP were prepared according to Beyer (1967). The NADH to DB electron-transfer activity was estimated by following the rate of NADH oxidized fluorimetrically (Krishnamoorthy & Hinkle, 1988). Protein estimation was done by Biuret method (Layne, 1957) in the presence of 0.4 mg/mL of potassium cholate. The complex-I activity was in the range of 0.10–0.15 μmol of NADH/min per mg of protein at 23 °C using DB as the electron acceptor.

Chemicals. ER and DODCI were purchased from Molecular Probes (Eugene, OR). Rotenone was purchased from Aldrich. Coupling of the decyl chain to the fifth position of 2,3-dimethoxy-6-methyl-1,4-benzoquinone to form DB and the subsequent purification was done according to Wan et al. (1975). Other chemicals used for the preparation of buffers were of analytical grade and the water was double distilled.

Methods. Steady-state fluorescence measurements were performed using a spectrofluorimeter (Model RF-540, Shimadzu Corp., Japan). The fluorescence lifetime measurements were performed using a CW mode-locked Nd-YAG laser-driven dye (Rhodamine 6G) laser system described elsewhere (Periasamy et al., 1988). The fluorescence decay curves were obtained using a time-correlated single photon counting set-up (Periasamy et al., 1988) coupled to a microchannel plate photomultiplier (Model 2809U, Hamamatsu Corp.). The samples were excited with (typically) 4-ps pulses from the dye laser, and the fluorescence emission was collected through either a 550-nm (in the case of ER) or a 590-nm (in the case of DODCI) cut-off filter followed by a monochromator. The cut-off filter was necessary because of high levels of scattering of the excitation beam from the particulate suspensions of membranous proteins. In fluorescence lifetime measurements, the emission was monitored at the magic angle (54.7°) to eliminate contribution from the decay of anisotropy. The half width of the excitation response function was ~100 ps (Bankar et al., 1989).

Since λ_{max} of absorption by ER is 520 nm, we used the 532-nm beam from the frequency-doubled output of the Nd-YAG laser which has a repetition rate of 82 MHz to excite the sample. In this case the repetition rate of the start pulse was 800 kHz. Due to this mismatch, the peak count obtained was very low. Hence the fluorescence decay data of ER had low S/N ratio. Therefore time-resolved fluorescence anisotropy decay measurements were not performed on the ER: complex-I system.

The fluorescence decay curves at the magic angle were analyzed by deconvolution with the excitation function (obtained using a purely scattering medium) to obtain the intensity decay function represented as a sum of two or three exponentials:

$$I(t) = \sum A_i e^{-t/\tau_i} \quad (i = 2 \text{ or } 3)$$

Analysis of the collected data to extract A_i and τ_i was done based on the iterative reconvolution method using nonlinear least-square and Marquardt algorithm for the optimization of parameters (Bevington, 1969).

The fluorescence anisotropy was measured by exciting the sample with vertically polarized laser pulse and collecting the fluorescence alternatively with the emission polarizer oriented either parallel or perpendicular to the direction of polarization of the exciting light. All the measurements were carried out at 23–25 °C.

For isotropic unhindered rotation of a fluorophore, the anisotropy $r(t)$ decays as a single exponential following an infinitely sharp excitation pulse

$$r(t) = r_0 e^{-t/\tau_r} \tag{1}$$

In eq 1, τ_r is the rotational correlation time of the fluorophore and r_0 is the initial anisotropy given by

$$r_0 = 0.4\{(3\cos^2\theta - 1)/2\}$$

(Lakowicz, 1983) where θ is the angle between the absorption and the emission dipoles of the fluorophore. The decay of the individual polarized components of the emission is given as

$$I_{\parallel}(t) = {}^1/_3 I_0(t)[1 + 2r(t)] \tag{2}$$

$$I_{\perp}(t) = {}^1/_3 I_0(t)[1 - r(t)] \tag{3}$$

where $I_0(t)$ is the decay of fluorescence intensity at magic angle. In the case of DODCI:complex-I system where there are two populations of DODCI, free and bound, the decay of the polarized components would be

$$I(t)_{\parallel} = \alpha\{{}^1/_3 e^{-t/\tau_1}[1 + 2r_1(t)]\} + (1 - \alpha)\{{}^1/_3 e^{-t/\tau_2}[1 + 2r_2(t)]\} \tag{4}$$

$$I(t)_{\perp} = \alpha\{{}^1/_3 e^{-t/\tau_1}[1 - r_1(t)]\} + (1 - \alpha)\{{}^1/_3 e^{-t/\tau_2}[1 - r_2(t)]\} \tag{5}$$

where $r_1(t)$ and $r_2(t)$ are the anisotropy of the two components with lifetimes τ_1 and τ_2, respectively, and α and $(1 - \alpha)$ are the fraction of the fluorescence intensity contributed by the two components. In our model, the anisotropy of the component with lifetime τ_1 is assumed to decay as $r_1(t)$ and that of τ_2 with $r_2(t)$. $r_1(t)$ and $r_2(t)$ are assumed to decay exponentially

$$r_1(t) = r_{01} e^{-t/\tau_{r1}}$$

$$r_2(t) = r_{02} e^{-t/\tau_{r2}} + r_\infty$$

where r_{01} and $(r_{02} + r_\infty)$ are the initial anisotropy values for

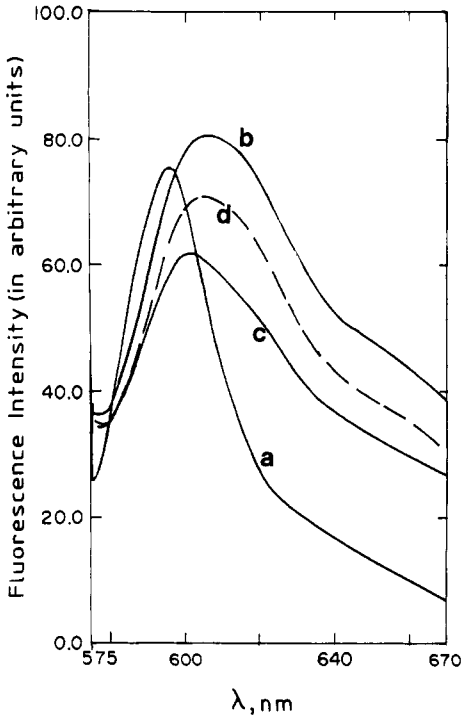

FIGURE 1: Binding of DODCI to complex-I and the effect of DB. The fluorescence emission spectrum of DODCI (20 nM) in sucrose buffer (250 mM sucrose, 10 mM MOPS, pH 7.5) was recorded by exciting at 560 nm (a). To this was added complex-I (0.18 mg mL^{-1}) and the emission spectrum recorded again (b). To see the effect of DB, 1 μM of DB was added to the above solution and the emission spectrum recorded (c). Addition of NADH (12 μM) to the above solution (DODCI:complex-I:DB) partially restored the higher fluorescence intensity (d).

the two components. The term r_∞ was included for the bound DODCI to take care of possible restricted rotational mobility of bound DODCI.

Experimentally measured polarized fluorescence decay data [$I_\perp(t)$ and $I_\parallel(t)$] are fitted simultaneously to eqs 4 and 5 to obtain best fit values for r_{01}, r_{02}, r_∞, τ_{r1} and τ_{r2}. Lifetimes of the two components were held fixed. Best fit criteria were (i) χ^2 value in the range of 0.8–1.2, (ii) random distribution of residuals, and (iii) agreement of calculated steady-state anisotropy with experimentally measured value. The above method of data analysis was tested using experimental data obtained from sample with known values of τ, r_0, and τ_r (Swaminathan & Periasamy, unpublished data). Other experimental details are given in the figure legends. Unless mentioned, all the experiments were performed at 23–25 °C.

RESULTS

Binding of DODCI to Complex-I. The cyanine dye DODCI binds to complex-I as shown by (i) a red shift of about 15 nm in the emission spectrum upon binding to complex-I and (ii) an increase in fluorescence intensity beyond 600 nm associated with spectral broadening (Figure 1). Addition of DB to a suspension of DODCI:complex-I decreased the fluorescence intensity beyond 600 nm. These changes, which are similar to those observed earlier in the case of ER (Ahmed & Krishnamoorthy, 1992), suggest that DODCI and DB share a common binding site on complex-I. The titration of DODCI with increasing concentrations of complex-I gave a hyperbolic curve (data not shown) similar to that obtained with ER (Ahmed & Krishnamoorthy, 1992). The dissociation constant obtained from this data was 55 nM, assuming 1:1 stoichiometry. Ultrafiltration experiments (Ahmed & Krishnamoorthy, 1992) also gave a similar value (64 nM) for the dissociation constant.

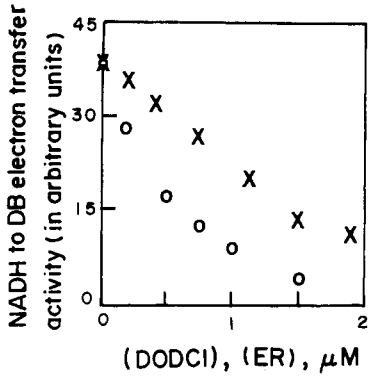

FIGURE 2: Inhibition of NADH to DB electron transfer activity of complex-I by either ER (×) or DODCI (○). The concentrations of complex-I and DB were 0.03 mg/mL and 5 μM, respectively.

Figure 2 shows the effect of binding of either ER or DODCI on the NADH to DB electron-transfer activity of complex-I. It can be seen that DODCI is about 2–3-fold more potent as an inhibitor when compared to ER. The difference between our inhibition data and those of a recent report on DODCI (Anderson et al., 1993) could be due to differences in the exponential conditions.

Fluorescence Lifetime of Complex-I-Bound DODCI and ER. Both DODCI and ER showed single exponential decay profiles in their free forms. Their lifetimes were ~700 (Das et al., 1993) and ~110 ps, respectively (Figure 3). In the presence of complex-I, the decay profiles of both the dyes could be analyzed as a sum of two exponentials (Figure 3). In both the cases one of the two lifetimes was close to that of the free form (Table 1). The other lifetime, which was significantly longer than that corresponding to the free form, could be assigned to the complex-I-bound dye. The lifetimes of the bound dyes were ~1.7 ns and ~600 ps in the cases of DODCI and ER, respectively (Table 1). The larger value of the mean lifetimes ($\tau_m = \Sigma\alpha_i\tau_i$) when compared to the lifetimes of the free dyes is in line with the increase in fluorescence intensity on binding. The amplitude corresponding to the bound form lifetime increased with the increase in the concentrations of complex-I (Figure 4). However the lifetimes themselves were not significantly dependent on the concentrations of complex-I (data not shown). Thus, the preexponential factors (amplitudes) could provide an accurate estimate of the level of dye binding. This could be especially very useful in turbid suspensions such as complex-I and submitochondrial particles where changes in the steady-state fluorescence intensity are often masked by changes in light scattering.

Effect of DB on the Fluorescence of Dye:Complex-I. Addition of DB, a widely used CoQ analogue (Krishnamoorthy & Hinkle, 1988), to a suspension of complex-I and either DODCI or ER resulted in a systematic decrease in A_2, the amplitude associated with the bound form (Table 1, lines 3 and 19). Subsequent addition of NADH to the above mixture resulted in relieving of the decrease in A_2 caused by DB (Table 1, lines 4 and 20). The time scale of this relieving effect by NADH matched with the rate of reduction of DB by NADH (data not shown). These results indicate that both the dyes (ER and DODCI) compete with DB for binding to complex-I. They also suggest that reduced DB does not replace the bound dye.

Apart from the above, in the case of DODCI:complex-I, addition of high concentrations of DB caused the appearance of a short (~0.15 ns) lifetime component (Table 1, line 10).

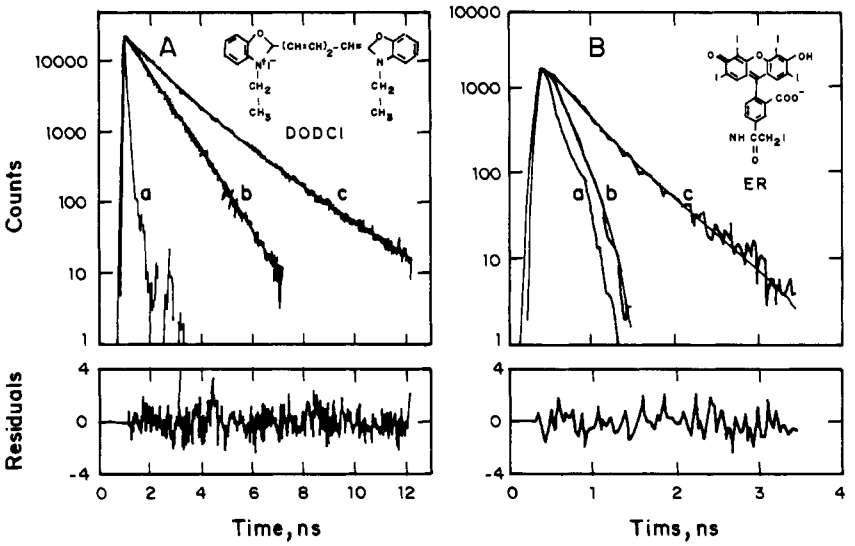

FIGURE 3: Fluorescence decay of DODCI (A) and ER (B) in the free form (traces b) and in the presence of complex-I (traces c). Traces a show the excitation profile. The concentrations used were as follows: ER, 0.20 μM; DODCI, 0.12 μM; complex-I, 0.15 mg mL^{-1} in the case of both ER and DODCI. The buffer used was 250 mM sucrose, 10 mM MOPS, pH 7.5. The excitation and emission wavelengths were 575 and 610 nm for DODCI and 532 and 560 nm for ER. The time-resolution was 37.8 ps/channel. The deconvoluted lifetimes are given in Table 1. Smooth lines in traces b and c are fitted curves.

Table 1: Fluorescence Lifetimes (τ_i) and Amplitude Factors (A_i) Measured in Dye:Complex-I Systems under Various Experimental Conditions

		fluorescence lifetime			normalized amplitude			
no.	sample	τ_1(ns)	τ_2(ns)	τ_3(ns)	A_1	A_2	A_3	χ^2
1	DODCI in buffer[a]	0.71	–	–	–	–	–	1.16
2	DODCI in complex-I[b]	0.84	1.79	–	0.35	0.65	–	0.98
3	-do- + DB (0.3 μM)	0.73	1.66	–	0.50	0.50	–	1.09
4	-do- + DB (0.3 μM) + NADH[c]	0.72	1.68	–	0.37	0.63	–	1.09
5	-do- + rotenone (0.5 μM)	0.84	1.93	–	0.37	0.63	–	1.10
6	-do- + DCCD (1 mM)	0.78	1.81	–	0.27	0.73	–	0.93
7	-do- + NADH (30 μM)	0.87	1.81	–	0.40	0.60	–	1.25
8	-do- + Ca^{2+} (3 mM)	0.73	1.70	–	0.76	0.24	–	1.04
9	-do- + DB (3.5 μM)	0.56	1.29	–	0.71	0.29	–	2.10
10	-do- + DB (3.5 μM)	0.72	1.47	0.14	0.60	0.16	0.24	1.16
11	-do- + DODCI (1.48 μM)	0.44	1.00	–	0.65	0.35	–	2.90
12	-do- + DODCI (1.48 μM)	0.64	1.31	0.14	0.67	0.07	0.26	1.13
13	-do- + DODA[d] (32 μM)	0.66	1.57	–	0.90	0.10	–	1.51
14	-do- + DODA (32 μM)	0.71	1.67	0.15	0.81	0.07	0.12	1.30
15	-do- at pH 5.0	0.70	1.75	–	0.81	0.19	–	0.94
16	-do- at pH 5.0	0.74	1.81	0.20	0.76	0.16	0.08	0.86
17	ER in buffer[a]	0.11	–	–	–	–	–	1.10
18	ER in complex-I[e]	0.14	0.57	–	0.83	0.17	–	0.85
19	-do- + DB (5 μM)	0.13	0.62	–	0.91	0.09	–	1.17
20	-do- + DB (5 μM) + NADH[c]	0.15	0.62	–	0.86	0.14	–	1.16
21	-do- + rotenone (0.5 μM)	0.13	0.54	–	0.83	0.17	–	1.19
22	-do- + DCCD (1 mM)	0.15	0.78	–	0.89	0.11	–	1.02
23	-do- + NADH (30 μM)	0.18	0.60	–	0.71	0.29	–	1.08
24	-do- + Ca^{2+} (1 mM)	0.17	0.59	–	0.75	0.25	–	1.20

[a] 250 mM sucrose, 10 mM MOPS, pH 7.5. [b] 0.15 mg/mL of complex-I and 120 nM of DODCI. [c] 40 μM. [d] Dodecylamine. [e] 0.15 mg/mL of complex-I and 200 nM of ER. The standard deviations in τ_i and A_i were less than 3%.

That the short lifetime component is not likely to be due to any possible quenching of fluorescence of bound DODCI by DB was shown by the following experiment. Long-chain amines such as dodecylamine, which are efficient inhibitors of electron flow from NADH to DB (Batayne et al., 1986, and also see later), also caused the appearance of the short component concomitant with a decrease in A_2 (Table 1, line 14). This suggests that the short lifetime is not likely to arise due to quenching of fluorescence of bound DODCI. It is likely that the short lifetime component is due to another binding mode of DODCI away from the DB binding site. The observation of the short lifetime component at very high levels of DODCI (Table 1, line 12) also suggest this model. These data also show that dodecylamine, DB, and DODCI share a common binding site.

Effect of Rotenone. Addition of rotenone to a suspension of complex-I and either DODCI or ER caused some minor changes in fluorescence decay profiles (Table 1, lines 5 and 21). These changes were mainly due to a slight but definite increase in the value of τ_2, the lifetime of the complex-I-bound DODCI. A_2 did not show any significant decrease indicating that rotenone did not displace the bound dye. The increase in τ_2 was consistently seen in a large number (~20) of DODCI:complex-I samples. In the case of ER:complex-I, τ_2 decreased slightly in the presence of rotenone (Table 1, line 21).

Effect of Reduction of Complex-I. Addition of NADH to a suspension of ER:complex-I resulted in an increase in the level of dye binding as revealed by the increase in A_2 (Table 1, line 23). A similar increase in A_2 was also observed when

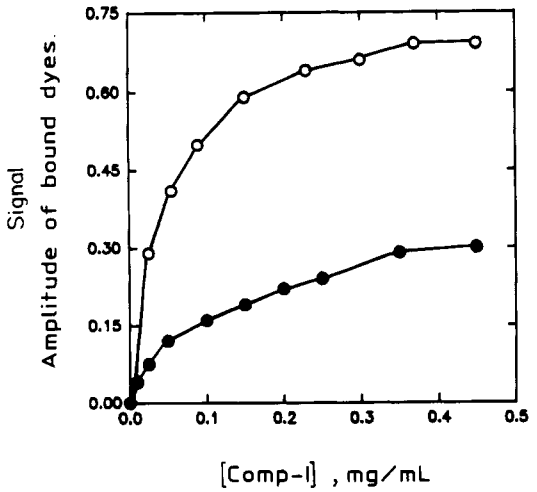

FIGURE 4: Dependence of the signal amplitude of complex-I bound dyes (A_2) on the concentration of complex-I. A_2 values were obtained from analysis of fluorescence decay curves by a sum of two exponentials (see methods). The concentrations of the dyes in sucrose buffer were 0.08 and 0.02 μM in the case of DODCI (○) and ER (●), respectively.

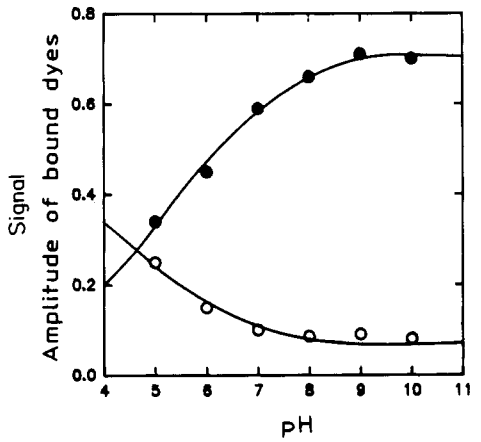

FIGURE 5: pH dependence of binding of DODCI (●) and ER (○) to complex-I. For DODCI:complex-I system, the sample contained 20 nM of DODCI and 0.20 mg mL^{-1} of complex-I in a mixed buffer (250 mM sucrose, 10 mM MES, 10 mM MOPS, and 10 mM Tris) at desired pH values. For ER:complex-I system, the sample contained 350 nM of ER and 0.13 mg mL^{-1} of complex-I. The amplitude values were obtained from double exponential analysis of the fluorescence decay curves.

the enzyme was reduced by dithionite (data not shown). In the case of the cationic dye, DODCI, the level of binding decreased in the presence of NADH as indicated by the decrease in A_2 observed in the presence of NADH (Table 1, line 7). In this case, the steady-state fluorescence intensity changes were largely masked by changes in light scattering by such perturbations. Hence these studies provide a representative example of how time-resolved fluorescence could be of help in observing small changes in equilibrium especially in turbid suspensions.

pH Dependence of Dye Binding. The binding of DODCI and ER to complex-I was pH dependent (Figure 5). The level of binding at the CoQ site increased with the increase in pH in the case of DODCI. The trend was reverse in the case of ER (Figure 5). These data suggest the involvement of titratable negative charge(s) in controlling the dye binding. The pH titration curves (Figure 5) indicate a pK_a in the range of ~6.5. The lifetime τ_2 of the bound dyes is largely pH insensitive (data not shown). In the case of DODCI, the decrease in the level of dye binding at the CoQ site at low pH values could be correlated with the emergence of the short

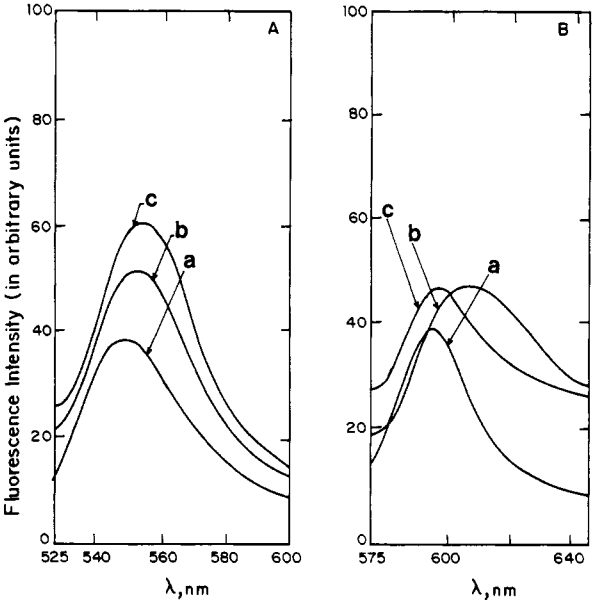

FIGURE 6: Effect of calcium on the fluorescence spectra of dye: complex-I. (A) The fluorescence spectrum of ER (340 nM) in sucrose buffer was recorded by exciting at 520 nm (a). To this sample was added 0.18 mg mL^{-1} of complex-I and the spectrum recorded again (b). Addition of calcium chloride (5 mM) increased the fluorescence intensity of ER:complex-I (c). (B) The emission spectrum of DODCI (110 nM) in sucrose buffer was recorded by exciting at 570 nm (a). To this was added 0.18 mg mL^{-1} of complex-I and the emission spectrum recorded (b). The spectrum c was recorded after the addition of 5 mM of calcium chloride.

lifetime (~0.20 ns) component (Table 1, line 16). This component, which was also seen in samples with high concentrations of DB (Table 1), could represent dye bound at a site other than the CoQ site.

Effect of Divalent Cations and Alkylamines and Acids. The nature of the dye binding site was probed by competition with hydrophilic (divalent cations) and hydrophobic (long chain alkylamines and fatty acids) agents. Divalent cations such as Ca^{2+} and Mg^{2+} had a significant effect on the dye binding. In the case of ER, the level of dye binding increased in the presence of Ca^{2+} whereas these divalent cations competed and expelled the bound cationic DODCI. This behavior was observed clearly both in time-resolved (Table 1, lines 8 and 24) and in steady-state measurements (Figure 6). These effects of Ca^{2+} were seen in SMP also (data not shown). Figure 7 shows the titration of fluorescence intensity of DODCI: complex-I with Ca^{2+}. It can be seen that the displacement of DODCI by Ca^{2+} (as shown by the decrease in the fluorescence intensity) is more efficient at high pH values. The dissociation constant K_{Ca} of Ca^{2+}–complex-I was obtained by fitting the change in fluorescence intensity (ΔF) on the total concentration of Ca^{2+} ($[Ca]_0$) according to the equation (Ahmed, 1993)

$$\Delta F = K_{Ca}[D]_0\Delta\phi/(K_d + K_{Ca}x)$$

where $x = [E]_0/(K_{Ca} + [Ca]_0)$, ΔF is the change in quantum yield on binding, K_d is the dissociation constant of DODCI: complex-I, and $[E]_0$ and $[D]_0$ are the total concentrations of complex-I and DODCI, respectively. Figure 8 shows the dependence of K_{Ca} with pH. The pH dependence of K_{Ca} is apparent from the raw data (Figure 7). The apparent pK_a of the pH dependence of K_{Ca} was ~6.

The observation that P-DB, which lacks the acyl chain of DB, was unable to compete with the dyes shows the hydrophobic nature of the dye binding site. This was further

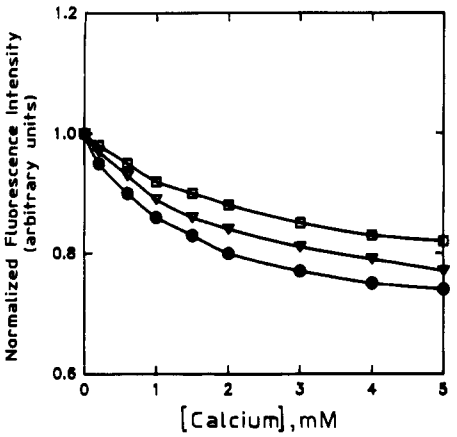

FIGURE 7: Dependence of fluorescence intensity of DODCI:complex-I on the concentration of Ca^{2+}. To a solution containing 24 nM of DODCI and 0.15 mg mL^{-1} of complex-I in mixed buffer (250 nM sucrose, 10 mM MES, 10 mM MOPS, and 10 mM Tris) was added increasing concentrations of Ca^{2+} and the fluorescence intensity recorded (excitation at 570 nm and emission at 610 nm). The fluorescence intensity of the solution before the addition of Ca^{2+} was taken as unity for normalization. The experiments were performed at pH 5.5 (□), pH 6.5 (▽) and pH 7.5 (●).

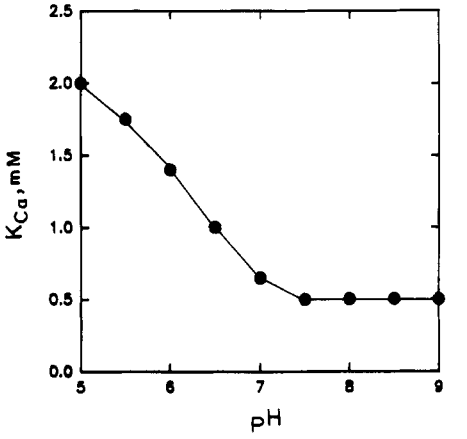

FIGURE 8: pH dependence of the dissociation constant of Ca^{2+}:complex-I. The dissociation constant (K_{Ca}) of Ca^{2+}:complex-I was determined from the effect of Ca^{2+} on the fluorescence intensity of DODCI:complex-I [see Figure 7 and Ahmed (1993)].

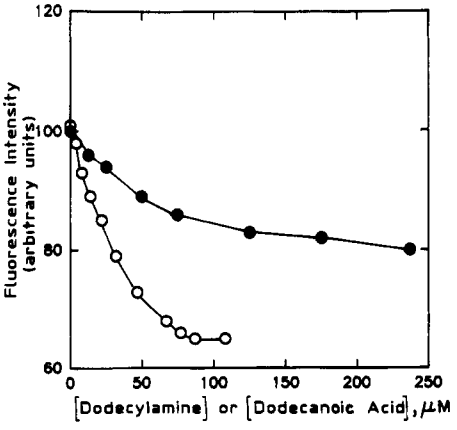

FIGURE 9: Dependence of the fluorescence intensity of DODCI:complex-I on the concentration of dodecylamine (○) and dodecanoic acid (●). To samples containing 80 nM of DODCI and 0.15 mg mL^{-1} of complex-I at pH 7.5 was added increasing concentrations of either dodecylamine or dodecanoic acid, and the fluorescence intensity was recorded.

confirmed by the effect of dodecylamine in competing with the bound DODCI (Figure 9). Also it could be seen that dodecanoic acid which was the same acyl chain is less effective in competing with the bound DODCI (Figure 9). The only difference between these two compounds is the charge on the functional group which is negative for dodecanoic acid and positive for dodecylamine at pH 7.5.

Effect of DCCD. The carboxyl group reagent DCCD has been shown to react with the energy transduction site in complex-I (Krishnamoorthy & Hinkle, 1988; Yagi, 1987). Treatment of complex-I with DCCD resulted in an increase in the level of binding of DODCI (Table 1, line 6). The increase in A_2 was observed throughout the pH range of 5–9, keeping the pH dependence still intact (data not shown). The effect of DCCD treatment of complex-I in ER:complex-I system was mainly on the lifetime of the bound ER. τ_2 increased significantly in DCCD treated samples (Table 1, line 22).

Fluorescence Anistropy Decay Measurements. In order to get information on the dynamic behavior of the bound dye, time-resolved fluorescence anisotropy was measured at a variety of conditions. Due to technical limitations (low S/N ratio and see Methods), these measurements were restricted to the DODCI:complex-I system only. The decay of fluorescence anisotropy of the DODCI:complex-I system could be analyzed as a sum of two exponentials, τ_{r1} and τ_{r2} (see Methods for the model). Typically the values of τ_{r1} and τ_{r2} were in the range of ~0.3 and 2–3 ns, respectively. The shorter component could be associated with the free DODCI in the aqueous medium and longer component to the complex-I-bound form (Table 2).

The anisotropy decay (rotational correlation time of the bound DODCI) showed a significant dependence on pH (Figure 10). Analysis showed that the shorter component (τ_{r1}) did not show any appreciable pH dependence. In contrast, τ_{r2} increased with the decrease in pH (Figure 10). Since the level of DODCI binding at the CoQ site was also pH dependent (Figure 5) and increased with increase in pH, there could be a correlation between these two pH dependences. In fact, the correlation between the level of dye binding (at CoQ site) and the apparent value of τ_{r2} was shown directly by the following experiment. In a titration where the concentration of complex-I was increased, keeping the concentration of DODCI constant, the value of τ_{r2} showed a systematic decrease from ~20 ns reaching a constant value of ~2–3 ns at high concentration of complex-I (Figure 11). Addition of DB to a suspension of DODCI:complex-I resulted in an increase in the value of τ_{r2} (Table 2). The rotational correlation time of DODCI bound at the CoQ site did not change significantly in the presence of rotenone (Table 2).

It was found that on reaction of complex-I with DCCD, the value of τ_{r2} almost doubled (Table 2). Treatment of sub mitochondrial particles (SMP) with DCCD also increased the rotational correlation time of DODCI bound to SMP (Table 2). The steady-state fluorescence anisotropy of complex-I:DODCI also showed an increase after DCCD treatment (Table 2). Thus these data suggest a correlation between the proton pumping activity and the level of rotational mobility of DODCI bound at the CoQ binding region of complex-I.

DISCUSSION

NADH:CoQ reductase is the least understood region of the mitochondrial electron transport chain. The lack of sufficient information concerns both the pathway of electron flow and the mechanism of the proton pump. Apart from answering the molecular mechanism of energy transduction in mitochondria, knowledge on the function of NADH:CoQ reductase is also important in explaining a variety of pathological

Table 2: Parameters Obtained from the Decay of Fluorescence Anisotropy in DODCI:Complex-I System

no.	sample	τ_1 (ns)	τ_2 (ns)	A_1	A_2	r_{01}	r_{02}	τ_{r1} (ns)	τ_{r2} (ns)	r_∞	χ^2	SSA[f]
1	DODCI in buffer[a]	0.71	–	–	–	0.33	–	0.31	–	–	1.17	–
2	DODCI in complex-I[b]	0.78	1.80	0.44	0.56	0.20	0.13	0.27	3.13	0.04	1.09	–
3	-do- + DB (5 μM)	0.69	1.58	0.86	0.14	0.37	0.06	0.16	>20	–	1.62	–
4	-do- + rotenone[c]	0.79	1.86	0.54	0.46	0.19	0.17	0.24	3.07	0.05	1.13	–
5	DODCI in complex-I[d]	0.78	1.82	0.39	0.61	0.20	0.12	0.15	3.03	0.05	1.29	0.25
6	-do- + DCCD (1 mM)	0.70	1.81	0.36	0.64	0.20	0.12	0.20	4.67	0.06	1.05	0.28
7	DODCI in SMP[e]	0.75	1.68	0.56	0.44	0.20	0.04	0.20	1.42	0.02	1.20	–
8	-do- + DCCD (1 mM)	0.73	1.64	0.45	0.55	0.26	0.07	0.17	5.38	0.01	1.09	–

[a] 250 mM sucrose, 10 mM MOPS, pH 7.5. [b] 0.15 mg/mL of complex-I and 20 nM DODCI. [c] 20 μg/mL of rotenone. [d] 0.25 mg/mL of complex-I and 30 nM DODCI. [e] 0.50 mg/mL of SMP and 30 nM DODCI. [f] Steady-state anisotropy.

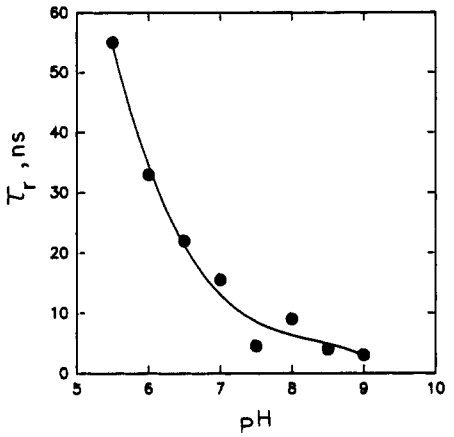

FIGURE 10: pH dependence of the rotational correlation time of complex-I-bound DODCI. The samples contained 0.15 mg mL^{-1} of complex-I and 80 nM of DODCI in mixed buffer at various pH values. The data was analyzed according to the model given in Methods to extract the rotational correlation time of bound DODCI. τ_r in the figure represents τ_{r2} in the analysis.

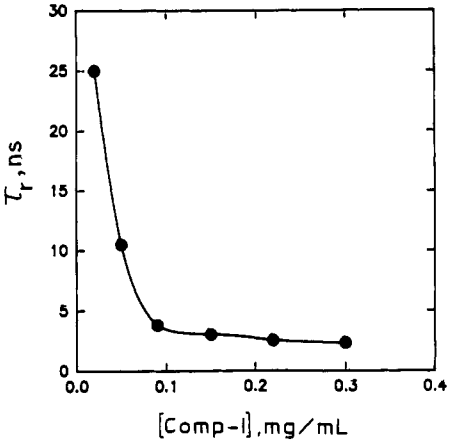

FIGURE 11: Dependence of rotational correlation time of bound DODCI on the concentration of complex-I. To sample containing 80 nM of DODCI at pH 7.5 was added varying concentrations of complex-I and the fluorescence emission collected. τ_r in figure represents τ_{r2} in the analysis.

conditions involving mitochondrial myopathy (Walker, 1992). In spite of limitations such as the huge molecular mass (700 kDa), a large number of subunits (>40), and the absence of convenient intrinsic probes, several studies (Weiss et al., 1991; Weiss & Freidrich, 1991) have shown that the proton pump of the enzyme complex is localized in the CoQ binding region. ATP-driven reverse electron flow experiments had indicated the region between low potential Fe–S centers and the CoQ as the site of energy coupling (Krishnamoorthy & Hinkle, 1988). Fluorescence studies using extrinsic probes are best suited for large membrane protein complexes such as complex-I. The present studies using fluorescence dynamics of probes bound to the CoQ region have shed some light on the nature of the putative H^+ pumping region of the enzyme complex.

Both the fluorescent probes DODCI and ER used in this work bind noncovalently to the CoQ binding region as shown by their displacement by DB (Figure 1 and Ahmed & Krishnamoorthy, 1992). However, displacement of bound probes by DB by an indirect mechanism cannot be ruled out. The stronger binding of DODCI ($K_d \sim 55$ nM) when compared to ER ($K_d \sim 0.15$ μM) could be due to stabilization of the positively charged DODCI by negatively charged protein side chains. The competition behavior of long-chain fatty acids and amines (Figure 9), which replace the bound DODCI, also support the above conclusion. In this case, the amine (with a positive charge on its functional group) was more potent in displacing bound DODCI when compared to acid (which has a negative charge on its functional group). The displacement of bound DODCI by Ca^{2+} (Table 1 and Figure 6) could also be due to electrostatic stabilization of either DODCI or Ca^{2+} by negative charge(s) in the binding site. The enhanced binding of negatively charged ER in the presence of Ca^{2+} (Table 1 and Figure 6) is also in lne with this picture. In this case, Ca^{2+} would reduce the electrostatic repulsion between ER and negatively charged side chains. That the bound dyes could be displaced by the hydrophobic DB (but not with P-DB which lacks the hydrophobic acyl chain) and long-chain fatty acids and amines (Figure 9) attests to the hydrophobicity of this region. Thus the CoQ binding region is largely hydrophobic with some hydrophilic residues as required by a proton pumping region.

The pH dependence of dye or Ca^{2+} binding (Figures 5 and 8) suggest that a group with pK_a ~6.5 could be responsible. The increased level of binding of either DODCI or Ca^{2+} with the increase in pH and the reverse behavior with ER suggest the involvement of carboxyl group(s). At high pH values (>6), the ionized carboxyl group could aid the binding of positively charged DODCI and destabilize the bound ER which has a negative charge. High pK_a values (~6) of carboxyl groups in hydrophobic environment have indeed been observed in many cases (Imoto et al., 1977; Rongey et al., 1993). Since carboxyl group(s) could be an element in conformationally linked proton pumps, it is attractive to associate these titratable groups to putative carboxylates in the CoQ binding region. The inhibition of this proton pump by carboxyl modifying reagent DCCD (Yagi, 1987) also implicate the involvement of carboxyl groups in proton pumping. DCCD has been shown to modify carboxyl group(s) in a 29-kDa subunit (Yagi & Hatefi, 1988). Recent studies (Heinrich et al., 1992) have indicated that the 9-kDa subunit which is involved in CoQ binding has conserved acidic residues.

Does the binding of Ca^{2+} in the CoQ/dye binding region have any physiological relevance? Kotlyar and Vinogradov (1990) have shown that the enzyme undergoes a slow active–inactive transition which is controlled by Ca^{2+}. The transition

from inactive to active form is dependent on enzyme turnover. Ca^{2+} and other divalent cations have been shown to inhibit this transition (Kotlyar et al., 1992). This transition was seen in the cases of both the forward (NADH to CoQ) and the reverse (succinate to NADH) electron transfer reactions. Kotlyar et al. (1992) have suggested that Ca^{2+} could be modulating the steady-state level of NADH oxidase activity inside the mitochondria. Our studies have provided further information in that this modulation could be the result of Ca^{2+} binding at the CoQ/dye binding site. The mitochondrial matrix is known to be one of the Ca^{2+} storage compartments in the cell (Carafoli, 1987). Hence, control of NADH oxidase activity by milimolar levels of Ca^{2+} is entirely plausible in the mitochondrial matrix. For Ca^{2+} to control the NADH oxidase activity, it is necessary that the binding site of Ca^{2+} be exposed to the matrix side of the inner membrane. Hence it is likely that the Ca^{2+} binding site in the CoQ region is exposed to the matrix (and NADH binding) side of NADH:CoQ reductase. Our observation that Ca^{2+} could modulate the level of dye binding in SMP (where the NADH binding site is exposed to the solvent) also shows that the binding site of Ca^{2+} is on the matrix side of the enzyme.

Our earlier steady-state observations on ER binding have shown that DB and the classical inhibitor rotenone do not share a common binding site (Ahmed & Krishnamoorthy, 1992). This result was quite contrary to earlier assumptions by many workers in this area. The present results from time-resolved fluorescence studies using DODCI and ER confirm the above conclusion. The small but definite increase in the value of τ_2 (Table 1), the lifetime of the bound DODCI, suggest a conformational change induced by rotenone resulting in a more hydrophobic environment of the bound dye. Conformational change induced by rotenone had been suggested by our earlier studies on the rapid kinetics of ER binding (Ahmed & Krishnamoorthy, 1992) and also cross-linking studies (Gondal & Anderson, 1985). The opposite effects on τ_2 of either DODCI:complex-I or ER:complex-I could be a reflection of the opposite charges on the two dyes (Figure 3). Such opposite effects were observed in other situations also (see later).

Reduction of the enzyme by either NADH or dithionite had resulted in an increase in the level of bound ER and a decrease in the level of bound DODCI (Table 1). Reduction-linked H^+ uptake in the dye binding region of complex-I could explain the above observations. It is attractive to speculate that the putative carboxyl group(s) implicated in the pH dependence of the level of dye binding could be the candidate involved in the reduction-linked protonation. Reduction-linked protonation of carboxyl group(s) would lead to a transition from negative charge to neutral at the dye binding site. This could, in turn, lead to a decrease in the level of binding of cationic DODCI and an increase in the level of binding of anionic ER. The relevance of such a picture is enhanced when we recognize that electron transfer linked H^+ release/uptake system is an essential element of a proton pump (Ragan, 1987).

The decay of fluorescence anisotropy of DODCI:complex-I has brought out some very interesting characteristics of the CoQ binding region. Firstly, the increase in the value of τ_{r2} (the rotational correlation time of the bound DODCI) with either the decrease in pH (Figure 10) or the increase in the value of [DODCI]/[complex-I] (Figure 11) needs discussion. It is likely that at high values of [DODCI]/[complex-I], DODCI binds to other nonspecific sites also apart from binding at the CoQ binding site which get saturated by the binding of DODCI. This was shown by the emergence of a new population under this condition (Table 1, line 12). The binding at the nonspecific site, which could be much weaker compared to binding at the CoQ site, could result in a large value of τ_{r2} reflecting the tumbling of the entire protein complex. When the concentration of complex-I is increased, the dye could be pulled from the nonspecific site(s) into the much stronger binding site at the CoQ region. This could be reflected in a lower value (2–3 ns) of τ_{r2} which could characterize the dynamics of DODCI bound at the CoQ site. Since the analysis of the anisotropy decay have been carried out based on a model with two populations only, the apparent values of τ_{r2} would represent a weighted average of various bound forms. Addition of DB had caused an increase in the value of τ_{r2}. Since DB and DODCI share a common binding site in the CoQ region, the observed increase in τ_{r2} cannot be due to perturbation of bound DODCI. It is likely that the DB-induced displacement of DODCI from the CoQ region could lead to binding of DODCI at the nonspecific site(s) mentioned above. Similar increase in τ_{r2} was also observed when the bound DODCI was displaced by dodecylamine (data not shown).

A rotational correlation time (τ_r) in the range of 2–3 ns for DODCI bound to the CoQ site suggests the presence of a high level of segmental mobility in that region. The τ_r associated with the tumbling of the entire complex-I molecule (with a molecular mass of ~700 kDa) is expected to be around 250 ns. When DODCI was bound at nonspecific and low-affinity sites, it did not have any appreciable rotational mobility with respect to the protein complex. In this case, the observed value of τ_r >20 ns would correlate with the overall tumbling of the protein complex. The observed lower value (~3 ns) of τ_r for DODCI bound at the high affinity CoQ binding site and the higher value (>20 ns) of τ_r for the dye bound at low affinity site(s) could appear counterintuitive. However, it is important to realize that there need not be any correlation between the affinity and the rotational mobility of a bound ligand (probe). A weakly bound ligand may be bound in such a way as not to have any mobility with respect to the macromolecule. Conversely, a high-affinity site such as CoQ binding site may have a high level of local segmental mobility resulting in an efficient rotational motion of the ligand. An alternative explanation for the low value (2–3 ns) of τ_r for DODCI bound at the CoQ site could be a partially hindered rotation without the involvement of local segmental mobility. However the modulation of τ_r of bound DODCI by DCCD support the segmental mobility as the cause of low value of τ_r of bound DODCI. Also in the case of hindered rotation of the probe, the rotational mobility is likely to approach that of the free probe in solution. The significantly high value of τ_r of bound DODCI (2–3 ns) when compared to that observed in free aqueous medium (~0.3 ns) also argues against a hindered rotation model.

Segmental mobility in a particular region has indeed been observed in several proteins (Jameson et al., 1987; Miki et al., 1982). However, these regions generally are solvent exposed and exterior surface of the proteins. Segmental mobility in a highly hydrophobic region such as the CoQ binding region appears rather unusual. However, if the CoQ binding region is the actual site of the proton pump, then a high level of segmental mobility would be a requirement rather than a coincidence. The importance of intramolecular motion in the functioning of enzymes is well documented (Karplus & Petsko, 1990). A redox-linked conformational change resulting in proton uptake (from one side of the membrane) would certainly

demand a highly flexible transmembrane segment. Assignment of the high level of segmental mobility with the proton pumping function is strengthened by the observation that reaction with DCCD, an inhibitor of the proton pump (Yagi, 1987), resulted in 2-fold increase in the value of τ_r (Table 2) and an increase in the steady-state anisotropy of the bound DODCI. Thus, a decrease in the segmental mobility could be correlated with the inactivation of the pump.

The effect of reaction with DCCD on the CoQ region was seen in other parameters also. The increase in the levels of binding of DODCI and the increase in the lifetime of bound ER also indicate large conformational changes. The observation of pH dependence of DODCI binding in DCCD-treated samples also suggest that the carboxyl group(s) which assist the binding of DCCD are not accessible to DCCD. Hence, the conformational changes could have been caused by reaction with other nearby carboxyl group(s).

ACKNOWLEDGMENT

We thank Prof. N. Periasamy for many valuable discussions and Dr. G. C. Joshi for his association in the early part of the experimental work involving ER.

REFERENCES

Ahmed, I. (1993) Ph.D. Thesis, University of Bombay.
Ahmed, I., & Krishnamoorthy, G. (1992) *FEBS Lett. 300*, 275–287.
Anderson, W. M., Wood, J. M., & Anderson, A. C. (1993) *Biochem. Pharmacol. 45*, 2115–2122.
Banker, K. V., Bhagat, V. R., Das Doraiswamy, S. R., Ghangrekar, A. S., Kamat, D. S., Periasamy, N., Srivatsavoy, V. J. P., & Venkataraman, B. (1989) *Indian J. Pure Appl. Phys. 27*, 416–428.
Batayneh, N., Kopacz, S. J., & Lee, C. P. (1986) *Arch. Biochem. Biophys. 250*, 476–487.
Bevington, P. R. (1969) in *Data Reduction and Analysis in Physical Sciences*, McGraw-Hill Inc., New York.
Beyer, R. E. (1967) *Methods Enzymol. 10*, 186–194.
Carafoli, E. (1987) *Annu. Rev. Biochem. 56*, 395–433.
Das, T. K., Periasamy, N., & Krishnamoorthy, G. (1993) *Biophys. J. 64*, 1122–1132.
Gondal, J. A., & Anderson, W. M. (1985) *J. Biol. Chem. 260*, 12690–12694.
Hatefi, Y., & Rieske, J. S. (1967) *Methods Enzymol. 10*, 225–239.
Heinrich, H., Azevedo, J. E., & Werner, S. (1992) *Biochemistry 31*, 11420–11424.
Hofhaous, G., Weiss, H., & Leonard, K. (1991) *J. Mol. Biol. 221*, 1027–1043.
Imoto, T., Johnson, L. N., North, A. C. T., Philips, D. C., & Rupley, J. A. (1977) in *The Enzymes* Vol. 7, (Boyer, P. D., Eds.) pp 665–858, Academic Press, New York.
Jameson, D. M., Gratton, E., & Eccleston, J. F. (1987) *Biochemistry 26*, 3894–3901.
Karplus M., & Petsko, G. A. (1990) *Nature 347*, 631–639.
Kotlyar, A. B., & Vinogradov, A. D. (1990) *Biochim. Biophys. Acta 1019*, 151–158.
Kotlyar, A. B., Sled, V. D., & Vinogradov, A. D. (1992) *Biochim. Biophys. Acta 1098*, 144–150.
Krishnamoorthy, G., & Hinkle, P. C. (1988) *J. Biol. Chem. 263*, 17566–17575.
Lakowicz, J. R. (1983) in *Principles of Fluorescence Spectroscopy*, Plenum Press, New York.
Laye, E. (1957) in *Methods Enzymol.* Vol. III (Colowick, S. P., & Kaplan, N. O. Eds.), pp 450–451, Academic Press, New York.
Lemasters, J. J., Grunwald, R., & Emaus, R. K. (1984) *J. Biol. Chem. 259*, 3058–3063.
Miki, M., Wahl, P., & Auchet, J. C. (1982) *Biochemistry 21*, 3662–3665.
Ohnishi, T. (1979) in *Membrane Proteins in Energy Transduction* (Capaldi, R. A., Ed.) pp 1–87, Marcel Dekker, New York.
Periasamy, N., Doraiswamy, S., Maiya, G. B., & Venkataraman, B. (1988) *J. Chem. Phys. 88*, 1638–1651.
Pilkington, S. J., Arizmendi, J. S., Fearnley, I. M., Runswick, M. J., Skehel, J. M., & Walker, J. E. (1993) *Biochem. Soc. Trans. 21*, 26–31.
Ragan, C. I. (1976) *Biochim. Biophys. Acta. 456*, 249–290.
Ragan, C. I. (1987) *Curr. Top. Bioenerget. 15*, 1–36.
Rongey, S. H., Paddock, M. L., Feher, G., & Okamura, M. Y. (1993) *Proc. Natl. Acad. Sci. U.S.A. 90*, 1325–1329.
Senior, A. E. (1979) *Methods Ezxymol. 55*, 391–397.
Tan, A. K., Ramsay, R. R., Singer, T. P., & Miyoshi, H. (1993) *J. Biol. Chem. 268*, 19328–19333.
Trumpower, B. L. (1990) *J. Biol. Chem. 265*, 11409–11412.
Tuschen, G., Sackmann, U., Nehls, U., Haiker, H., Buse, G., & Weiss, H. (1990) *J. Mol. Biol. 213*, 845–857.
Walker, J. E. (1992) *Q. Rev. Biophys. 25*, 253–324.
Wan, Y. P., Williams, R. H., Folkers, K. H., & Racker, E. (1975) *Biochem. Biophys. Res. Commun. 63*, 11–15.
Wang, D. C., Meinhardt, S. W., Sackmann, U., Weiss, H., & Ohnishi, T. (1991) *Eur. J. Biochem. 197*, 257–264.
Weiss, H., & Freidrich, T. (1991) *J. Bioenerget. Biomembr. 23*, 743–754.
Weiss, H., Freidrich, T., Hofhaus, G., & Preis, D. (1991) *Eur. J. Biochem. 197*, 563–576.
Wikstrom, M. (1984) *FEBS Lett. 169*, 300–304.
Yagi, T. (1987) *Biochemistry 26*, 2822–2828.
Yagi, T. (1990) *Arch. Biochem. Biophys. 281*, 305–311.
Yagi, T., & Hatefi, Y. (1988) *J. Biol. Chem. 263*, 16150–16155.